Supplementary Information [SI]

Characterizing Thalamo-cortical Disturbances in Schizophrenia and Bipolar Illness

Alan Anticevic[1,2,3], Michael W. Cole[4], Grega Repovs[5], John D. Murray[6,7], Margaret S. Brumbaugh[8], Anderson M. Winkler[1,8,9], Aleksandar Savic[1,3,10], John H. Krystal[1,2,3], Godfrey D. Pearlson[1,6,8], David C. Glahn[1,8]

1. Department of Psychiatry, Yale University School of Medicine, 300 George Street, New Haven, CT 06511, USA
2. NIAAA Center for the Translational Neuroscience of Alcoholism, New Haven, CT 06519, USA
3. Abraham Ribicoff Research Facilities, Connecticut Mental Health Center, New Haven, CT 06519, USA
4. Department of Psychology, Washington University in St. Louis, St. Louis, MO 63130, USA
5. Department of Psychology, University of Ljubljana, Ljubljana, Slovenia
6. Department of Neurobiology, Yale University, 333 Cedar St., New Haven, CT 06510, USA
7. Department of Physics, Yale University, New Haven, CT 06510, USA
8. Olin Neuropsychiatry Research Center, Institute of Living, Hartford Hospital, 200 Retreat Avenue, CT 06106, USA
9. Oxford University, John Radcliffe Hospital, Headington, Oxford OX3 9DU, UK
10. University Psychiatric Hospital Vrapce, University of Zagreb, Zagreb 10000, Croatia

Corresponding Author:

Alan Anticevic Ph.D., Yale University, Department of Psychiatry
34 Park St., New Haven, CT 06519, Office (203) 974-7763
alan.anticevic@yale.edu

Key Words: thalamus; schizophrenia; connectivity; resting-state; bipolar illness

SI Methods

Inclusion Criteria for the Schizophrenia Discovery Sample. Patients were identified through outpatient clinics and community mental health facilities in the Hartford (CT) area. Inclusion criteria for patients were: i) schizophrenia diagnosis as determined by the Structured Clinical Interview (SCID) for the Diagnostic and Statistical Manual of Mental Disorders-IV (DSM-IV) (First et al. 2002), administered by experienced MA or PhD-level research clinicians; ii) no history of major medical or neurological conditions (e.g. epilepsy, migraine, head trauma with loss of consciousness); and iii) IQ>70 assessed by widely-accepted methods for estimating premorbid intelligence levels [either National Adult Reading Test (NART), Wide Range Achievement Test (WRAT) or Wechsler Test of Adult Reading (WTAR) depending on the study protocol] (Spreen and Strauss 1998). All measures were appropriately normed and converted to IQ equivalents for each subject. If more than one premorbid achievement measure was available per subject the scaled scores were averaged per standard practice. We conducted two follow up analyses to better characterize the role IQ may play with respect to our findings: i) We used IQ as a covariate; and ii) we correlated IQ in patients only with the severity of altered over/under connectivity findings. When used as a covariate, IQ did not explain any significant variance, nor did it alter the magnitude of the between-group effects for over or under-connectivity effects reported in the main text. Moreover, IQ did not significantly correlate with either over or under-connectivity effect in patients (r=-.12, p=.26; and r=.08, p=.45 for over and under-connectivity respectively, both 2-tailed). Of note, given the sample size (N=90) were adequately powered to detect meaningful effects (well over 80% power for medium-moderate effects between identified connectivity and IQ) and neither approached even a trend-level effect. Finally, to further rule out the possibility that differences on the used IQ measures drove the effects, we computed a follow up analysis where we selected a sub-sample of N=73 patients and controls explicitly matched on IQ as well as all other variables. We re-computed the main effect t-test for these IQ-matched samples (Figure S14), which revealed the same patter of results. Nonetheless, it is important to note that the 'IQ' measures used here may not reflect the complex nature of cognitive deficits in schizophrenia, which may relate to presently observed thalamic findings (Parnaudeau et al. 2013).

As done in our prior work (Anticevic et al. 2012), to increase generalizability of the patient sample, co-morbid Axis I anxiety disorders and/or history of substance abuse (fully remitted >6 months prior to the study) were allowed (although prior substance abuse is a complex issue in schizophrenia and requires prospective investigation (Krystal et al. 2006), see Limitations). Healthy participants were recruited through media advertisements and flyers posted in the Medical Center area. Inclusion criteria for healthy participants were: i) no current or lifetime Axis I psychiatric disorder as assessed by SCID-NP; ii) no history of medical or neurological conditions; and iii) no history of psychotic disorders in first-degree relatives (reported by detailed family history). We additionally examined 67 patients diagnosed with bipolar I illness and 47 matched controls. Moreover, we replicated key schizophrenia findings in a well-characterized smaller sample of schizophrenia patients (N=23) and matched healthy controls (N=23), diagnosed independently at a different site (Washington University in St. Louis, St. Louis, MO). Detailed inclusion/exclusion criteria for the bipolar and schizophrenia replication samples are provided in our prior work (Anticevic et al. 2011; Cole et al. 2011; Anticevic *et al.* 2012). Nonetheless, for completeness, we present demographics for bipolar and schizophrenia replication clinical samples in **Tables S3-4**. As noted in the main text, all analyses presented here were orthogonal to any prior reported effects using the replication and bipolar samples.

Missing Values Imputation for the Schizophrenia Discovery Sample. Originally, we assembled a database of 111 patients diagnosed with schizophrenia and 269 healthy control subjects with available BOLD data (selection was based on signal-to-noise (SNR) parameters and head movement characteristics). Of the overall sample, 11 patients and 7 controls were missing information on maternal education and further 13 patients and 2 controls were missing paternal education information. To accomplish appropriate group matching we imputed missing values for these relevant demographic characteristics based on the available sample, as is standard statistical practice (Gelman and Hill 2007). Imputing was done in two steps: i) Maternal education was predicted using a linear regression model including paternal education, age of the subject and subject's educational level as predictors. The model yielded adjusted R^2 of 0.4933 and was used to impute missing values. Models that included additional variables (experimental group, age) did not significantly improve regression and were not used. ii) Maternal and paternal education were predicted separately using subject's age and education. The models yielded adjusted R^2 of 0.1356 and 0.1748 for predicting maternal and paternal education respectively. Missing values were then replaced by relevant model-predicted values. Five

patients and one control subject were missing all information on education and were excluded from data imputation (i.e. these participants did not receive imputed values and were not used for further analyses).

Group Matching for the Schizophrenia Discovery Sample. For optimal group matching, several variables were used to find most similar pairs of subjects from each group. Specifically, gender and handedness were converted to numeric values coding 1 for female, 2 for male, 1 for right handedness, 2 for left handedness and 1.5 for ambidextrous subjects. All six variables (gender, handedness, subject age, maternal and paternal education, and average imaging signal-to-noise (SNR)) were then standardized across all subjects to mean of 0 and standard deviation of 1 to ensure equal weighting. We divided values for maternal and paternal education by a value of 2. This was done to accomplish joint educational level, which is equally weighted as other variables. Additionally, due to relatively larger between-group variability, SNR z-scores were multiplied by 2 to ensure better matching on SNR – deemed a critical variable in neuroimaging case-control studies (Parrish et al. 2000; LaBar et al. 2001). Distances between all possible pairs of patients and controls were then computed as Euclidian distances in the 6 dimensional space defined by matching variables. Pairs were sorted from smallest to largest distance and each patient was matched with the most similar control subject. Following matching, 14 more patients were excluded due to insufficient information on clinical characteristics, necessary for individual differences analyses. Finally, two remaining patients without relevant demographic information were also excluded. This yielded a total sample of 95 participants per group with available demographic and clinical characteristics. In addition, 5 more subjects per group were flagged based on rigorous movement criteria(Power et al. 2012) (see Data Preprocessing and Analysis section), resulting in a final well-matched sample of N=90 per group (**Table 1**), constituting one of the largest resting-state schizophrenia samples to date. Next, the resulting pairing was tested for between-group differences confirming that the two groups did not significantly differ on any of the matching variables (see **Table 1**), except for education attainment and premorbid intellectual functioning, which was lower for patients, and likely reflects the shortened educational achievement for patients due to illness onset (Glahn et al. 2006). Also, education differences are impacted by the illness course (Goldman-Rakic 1995) and thus were not included as a covariate. However, alcohol/drug use, age, gender and medication did not alter reported effects (see Limitations for a comprehensive discussion of 3rd variable issues across samples). More specifically, to rule out medication effects, we computed chloropromazine (CPZ) equivalents for each patient (Andreasen et al. 2010) across both discovery and replication schizophrenia samples. We used this CPZ variable as a co-variate. This did not alter our effects. Moreover, the two schizophrenia samples that were recruited across different sites received somewhat different levels of mediation doses (as reflected by a different CPZ equivalent mean level). Yet, the key effects replicated across samples with comparable effect sizes (see **Figure 2**). Collectively, these results are inconsistent with medication being a major confound in our analyses. Nonetheless, medication remains a key consideration for follow up studies (see Limitations for more detail).

Thalamic Clustering and Dysconnectivity Analyses. Thalamic clustering was accomplished in a multi-step method optimized to deal with individual differences in thalamic anatomy (which is not a problem when examining segmented thalamus as a whole for each subject): i) we identified all thalamic voxels using FreeSurfer segmentation, ii) we identified the subject with the most similar thalamic segmentation to the group as a whole and used this individual's thalamic segmentation as a template for non-linear registration of all thalamic voxels across all subjects (ignoring all other voxels). This was done to minimize across-subject differences in thalamic shape and size (although prior reports suggest subcortical alignment may not be as much of an issue in schizophrenia case-control studies (Anticevic et al. 2010)). Registration was accomplished via FSL's well-validated functional non-linear image registration tool (FNIRT) (Klein et al. 2009). We acknowledge there are many ways to accomplish this step; nonetheless, the chosen approach is well-validated and produced robust effects across cluster solutions; iii) next we applied the non-linear transformation matrix to BOLD image voxels that correspond to individually segmented thalamic volumes. Subsequently, we computed seed-based fcMRI for each thalamic voxel with all other gray matter voxels within a given subjects' brain (gray matter mask was defined based on FreeSurfer cortical segmentation codes where at least 25% of all subjects had gray matter to ensure gray matter signal is adequately captured, similar to our prior approaches (Cole *et al.* 2011; Anticevic *et al.* 2012)). This way we obtained a comprehensive voxel-wise gray matter connectivity map of each voxel in the thalamus for each subject. Next, we applied a Fisher r-to-Z transform to the subject-specific thalamic connectivity maps and then computed group average connectivity maps for each thalamic voxel for each group separately (see **Figure S8** for a conceptual visual illustration of the workflow). Next, we

computed a group difference map and obtained dysconnectivity maps for each thalamic voxel. We then used this difference map as the input to *k*-means clustering, as validated in prior work (see **Figure S8**). Specifically, whole-brain dysconnectivity maps were converted to one-dimensional vectors and used to compute correlation between each pair of thalamic voxels, where the correlation reflected the similarity of dysconnectivity between two voxels across the whole brain. 1-r was then used as a dissimilarity measure and *k*-means clustering algorithm was applied to find *k* number of clusters that group together the voxels with most similar dysconnectivity patterns across the brain between the two groups. To minimize the possibility of the algorithm being caught in a local minima, the clustering for each k was repeated 10 times with different random starting values and the solution with the smallest within-cluster distances was accepted (Nanetti et al. 2009; Cauda et al. 2011).

The overarching aim of this analysis was to ascertain if the thalamus could be segregated into specific regions with different patterns of dysconnectivity, which might individually contribute to (or even cancel each other out) when studying dysconnectivity of thalamus as a whole. With that in mind, a significant question when using *k*-means clustering is what number of clusters to search for? In the context of this study, the central question is how many thalamic sub-divisions with specific patterns of dysconnectivity can we expect to find in schizophrenia? We acknowledge that this is a difficult assumption to make a priori; especially since no comprehensive data-driven thalamic dysconnectivity investigation was previously attempted in schizophrenia. For this reason we have examined a number of *k* values and show both 4 and 6 cluster solutions (**Figures S9-10**). Critically, regardless of the choice of clustering solution we found that the pattern of group differences converged around a specific thalamic cluster that follows thalamic anatomy (see **Figure 4** and **Figure 9-11**).

To further specify the extent of thalamic dysconnectivity in schizophrenia, we explicitly examined, which voxels within the thalamus may show the largest group differences in the pattern of functional connectivity with the rest of the brain. To assess the differences between each group's average voxel-wise thalamic seed-map via a single value, we made use of the eta^2 index that quantifies the pattern of similarity between two signals, or in this case functional images (where eta^2 is designed to vary from 0 for no similarity to 1 for perfect signal similarity; for further detail see (Cohen et al. 2008)). That is, the employed method was explicitly designed to capture similarity (eta^2) or dissimilarity (1- eta^2) between a pair of functional connectivity maps (Cohen *et al.* 2008). As accomplished when computing the 1-r value to perform clustering, we converted the Fz group seed-maps to one-dimensional vectors for each thalamic voxel for which we computed 1-eta^2. This captured the dissimilarity between patient and control group average seed-maps for that specific thalamic voxel. The advantage of using 1-eta^2 in this case is that whereas 1-r reflects only the dissimilarities in the pattern of connectivity, 1-eta^2 captures also possible differences in the connectivity strength for voxels with similar connectivity patterns. In that sense, 1-eta^2 captures the overall 'dissimilarity' between two connectivity maps – in this case the difference between patients vs. control thalamo-cortical connectivity:

$$1 - eta^2 = 1 - (1 - \frac{\sum_{i=1}^{n}[(a_i - m_i)^2 + (b_i - m_i)^2]}{\sum_{i=1}^{n}[(a_i - \bar{M}_i)^2 + (b_i - \bar{M}_i)^2]}$$

As described in detail by Cohen and colleagues (Cohen *et al.* 2008), here *ai and bi* correspond to connectivity at position *i* (in this case a given voxel in the thalamus) for maps *a* and *b* respectively (in this case patient vs. control thalamo-cortical connectivity). *mi* corresponds to the mean value of the two images at position *i*, (*ai*+*bi*)/2. M-bar represents the grand mean value across the mean image (designated by *m*). By computing, 1-eta^2 for each thalamic voxel we generated a gradient map of 'dis-similarity' in thalamic functional connectivity between the two groups (see **Figure 5B**) for which highest 1-eta^2 values identify voxels with largest between-group differences in thalamo-cortical coupling. Moreover, such a map can be readily juxtaposed with both cluster-based and anatomically-derived thalamic nodes to provide a quantitative guide regarding thalamic sectors showing greatest dysconnectivity in schizophrenia (**Figure 5A-B**).

Anatomy-based Thalamic Connectivity Analyses. Above approaches examined the entire thalamus (defined on subject-specific thalamic anatomy) or used data-drive techniques. This was done to quantify the overall between-group effect, identify clusters of between-group differences in thalamic subdivisions, as well as compute a data-driven dysconnectivity gradient based on a between-group dis-similarity in thalamo-cortical connectivity. However, as noted, a key question pertains to whether these results follow known thalamic anatomy. To this end, we provide another complimentary analysis based on a priori anatomically delineated

thalamic subdivisions that were obtained using human cortical tractography (Behrens et al. 2003; Johansen-Berg et al. 2005). Specifically, we used the probabilistic thalamic atlas freely available in FSL, from which we derived thalamic anatomically-defined seeds. For completeness, we provide: i) a qualitative comparison with results above, to allow inspection of anatomical source of dysconnectivity (**Figure 5**); ii) a seed-based computation of between-group differences for each of the a priori defined anatomic thalamic subdivisions (**Figure S10**); iii) a formal quantitative comparison of similarity (using eta^2) between each anatomically-derived and clustering-identified map of dysconnectivity (**Figure S11**). The logic here was to demonstrate that the clustering-derived differences centered on thalamic subdivisions that may project to prefrontal cortex were indeed most similar to seed-maps derived when using an a priori thalamic seed known to project densely to prefrontal cortex.

Group Classification Using Multivariate Pattern Analysis (MVPA). We used linear support vector machines with LIBSVM in MATLAB (Chang and Lin 2011) [Software available at http://www.csie.ntu.edu.tw/~cjlin/libsvm] to test the consistency of thalamic dysconnectivity on an individual subject basis. The key utility of this additional classification analysis was to provide provisional evidence that observed disrupted thalamic connectivity might aid diagnostic decisions and may be sensitive to predicting group membership. Each subject's preprocessed whole-brain voxel-wise map of thalamic connectivity (used for the above analyses) was preprocessed further using a standard approach for MVPA: removing voxels that were 0 for any subject and z-normalizing each voxel (removing each subject's across-voxel mean and dividing by each subject's across-voxel standard deviation). Standard leave-one-subject-out cross-validation was then used to train and test the linear support vector machines (C=1) using the preprocessed data. In other words, each subject was held out in turn as their group membership (patient or control) was predicted based on a support vector machine trained to distinguish the groups based on the other subjects' data. This was done across all patient and control subjects relative to their original groups.

A lack of balance could be problematic for these analyses, since it could bias a classifier to predict that any input data more likely belonged to one group over another. The schizophrenia discovery (N=90/90, total N=180) and schizophrenia replication (N=23/23, total N=46) datasets were already balanced, and so the entire datasets were included in the classification analyses. By contrast, the bipolar patient dataset was not balanced (N=67/47). Therefore, a randomly sampled subset of 47 patients relative to 47 controls was selected for inclusion. Statistical significance for all classifications was obtained using permutation testing (1000 permutations per analysis). Identical methods as the original analyses were used for the permutations, except that the labels were randomly permuted (using MATLAB's *randperm* function) prior to training and testing. Each p-value was obtained based on the frequency of permutation-based accuracies above the empirically observed accuracy. Note that p=.001 was the smallest p-value possible given that 1000 permutations were used per analysis.

Overview of Bipolar Analyses. We conducted a number of analyses for the bipolar patient sample (**Table S3**) to characterize the nature of the defined disturbance schizophrenia. We studies bipolar illness given that it may share risk factors with schizophrenia, and could potentially reflect shared neural system disturbances. However, bipolar illness may also differ in important ways from schizophrenia. To this end, we computed the following analyses to shed light on both similarities and differences across these diagnoses: i) We computed threshold-free thalamic functional connectivity patterns displayed for the bipolar patient sample only to allow a qualitative comparison to other groups (**Figure S1**); ii) We provide a direct comparison between bipolar patients and their respective matched controls (**Figure S2E**). These results are presented following TFCE correction within the mask of regions showing group differences for the discovery schizophrenia sample (given statistical independence); iii) We also present the between-group threshold-free surface contrast map for the bipolar sample to allow complete interpretation of results (**Figure S2F**); iv) We computed the distributions of thalamo-cortical connectivity for the bipolar sample within the regions identified by the schizophrenia discovery sample (**Figure S3**) to assess the magnitudes of this effect across diagnoses; v) We compute the between-group thalamic connectivity contrast maps for schizophrenia vs. bipolar patients (**Figure S4**) to explicitly identify regions where there may be differences between the two groups; vi) We computed the relationship between thalamic over & under-connectivity in bipolar Illness, which was extracted out of regions identified in the schizophrenia discovery sample. These results are presented both in the main text (**Figure 3**) as well as more comprehensively in the Supplement (**Figure S7**); vii) Finally, we computed the MVPA-based diagnostic classification for bipolar patients, which were presented in the main text along with schizophrenia

results (**Figure 6**). These analyses shed light regarding the usefulness of identified connectivity alterations in diagnoses across psychiatric categories with shared features.

SI Figures

Table S1 | Regions showing reduced thalamic fcMRI for schizophrenia (N=90) patients vs. healthy controls (N=90)

X	Y	Z	Hemisphere	Anatomical Landmark	Peak T Statistic	Size (cubic mm)
-1	-16	8	Left	medial dorsal nucleus	5.79	2970
19	-71	-31	Right	cerebellum	5.62	4212
7	-63	-45	Right	cerebellum	5.56	4023
-10	-62	-34	Left	cerebellum	5.55	4104
15	-20	37	Right	cingulate gyrus	5.38	1809
-2	-82	-31	Left	cerebellum	5.37	4212
48	28	32	Right	middle frontal gyrus	5.26	1539
34	-52	-44	Right	cerebellum	5.08	2916
-39	-55	-45	Left	cerebellum	5.06	3402
-24	-9	-6	Left	lateral globus pallidus	5.01	2970
-44	25	37	Left	middle frontal gyrus	4.94	2025
26	37	44	Right	superior frontal gyrus (BA 8)	4.85	2133
-5	21	43	Left	medial frontal gyrus	4.83	3618
-17	6	16	Left	caudate	4.80	1701
31	52	24	Right	superior frontal gyrus (BA 10)	4.57	2943
25	-16	-6	Right	lateral globus pallidus	4.55	1269
-17	-44	-44	Left	cerebellum	4.44	3780
41	11	49	Right	middle frontal gyrus	4.43	2349
23	7	1	Right	putamen	4.29	1674
-33	51	24	Left	middle frontal gyrus	4.24	2052
-10	-10	27	Left	cingulate gyrus	4.24	2538
16	-44	-29	Right	cerebellum	4.03	3537
-2	-25	-17	Left	midbrain	3.94	2511
-25	12	54	Left	superior frontal gyrus	3.93	2052
-19	-28	33	Left	cingulate gyrus (BA 31)	3.89	1863
-30	-84	-39	Left	cerebellum	3.89	2700
43	-72	-38	Right	cerebellum	3.88	2187
-23	-101	-15	Left	lingual gyrus	3.87	1242
10	-38	-50	Right	cerebellum/brain stem	3.81	1404
50	-10	-38	Right	inferior temporal gyrus (BA 20)	3.77	1350
31	-88	-31	Right	cerebellum	3.70	1998
6	-99	-12	Right	lingual gyrus (BA 18)	3.69	945
-15	-42	-23	Left	cerebellum	3.62	1971
-6	38	20	Left	anterior cingulate (BA 32)	3.57	1593
8	9	20	Right	caudate	3.53	1755
21	-38	26	Right	sub-lobar, extra-nuclear white matter	3.16	1053
14	12	48	Right	superior frontal gyrus	3.12	1323
-33	12	-5	Left	insular cortex (BA 13)	2.91	1647
1	53	40	Right	medial frontal gyrus (BA 9)	2.73	783
-29	-35	-1	Left	hippocampus tail	2.61	486

Table S1. Region Coordinates Showing Reduced Thalamic Connectivity for Schizophrenia Patients (N=90) vs. Healthy Controls (N=90).

Table S2 | Regions showing increased thalamic fcMRI for schizophrenia (N=90) patients vs. healthy controls (N=90)

X	Y	Z	Hemisphere	Anatomical Landmark	Peak T Statistic	Size (cubic mm)
54	-34	10	Right	superior temporal gyrus	6.35	3996
38	-27	55	Right	postcentral gyrus	5.78	3645
-20	-79	22	Left	cuneus	5.55	3564
-50	-43	11	Left	superior temporal gyrus	5.55	3942
34	-7	7	Right	insular cortex	5.30	1620
-50	-10	26	Left	precentral gyrus	5.29	3915
-40	-27	56	Left	postcentral gyrus	5.28	3510
49	-11	30	Right	precentral gyrus	5.08	3807
6	-49	68	Right	post-central gyrus (BA 7)	4.90	1350
18	-77	26	Right	cuneus	4.87	3186
18	-57	-2	Right	lingual gyrus	4.85	3375
10	-21	74	Right	precentral gyrus	4.50	2187
-50	-15	-1	Left	superior temporal gyrus	4.43	2646
-48	23	14	Left	inferior frontal gyrus	4.43	1188
-17	-57	-9	Left	cerebellum	4.34	2565
31	-29	18	Right	posterior insular cortex (BA 13)	4.28	1890
0	-24	51	Midline	medial frontal gyrus (BA 6)	4.18	2268
-16	-19	74	Left	precentral gyrus	3.96	2241
22	-76	-11	Right	cerebellum	3.76	1215
-24	-77	-16	Left	cerebellum	3.73	1890
38	6	25	Right	inferior frontal gyrus (BA 9)	3.61	1053
-41	-73	-2	Left	middle occipital gyrus	3.48	2295
-42	-31	27	Left	inferior parietal lobule	3.47	1080
-16	-41	8	Left	posterior cinguate (BA 29)	3.46	1161
50	-10	-8	Right	middle temporal gyrus	3.43	2214
48	-72	-7	Right	middle occipital gyrus	3.35	2133
16	-38	7	Right	posterior cinguate (BA 29)	3.30	1323
34	-83	12	Right	middle occipital gyrus	3.12	810
24	-61	46	Right	precuneus	3.12	1215
-19	-43	69	Left	postcentral gyrus	3.03	756
39	-56	10	Right	superior temporal gyrus (BA22)	2.78	1458
25	-4	64	Right	superior frontal gyrus (BA 6)	2.70	675
53	14	-11	Right	superior temporal gyrus (BA 38)	2.43	351

Table S2. Region Coordinates Showing Increased Thalamic Connectivity for Schizophrenia Patients (N=90) vs. Healthy Controls (N=90).

Table S3 | Clinical and Demographic Characteristics - Bipolar Sample

Characteristic	Controls (N=47)		Patients (N=67)		Significance	
	M	S.D.	M	S.D.	T Value / Chi-Square	P Value (two-tailed)
Age (in years)	30.98	10.28	31.99	11.49	.48	.63
Gender (% male)	42.55		29.85		1.39	.16
Paternal education (in years)	12.79	3.92	14.95	3.61	3.02*	<.01
Maternal education	13.47	2.55	14.06	2.66	1.18	.23
Participant's education (in years)	15.28	2.11	14.16	1.81	3.01*	<.01
Clinical Course						
Age at Diagnosis	-	-	17.98	6.10	-	-
Duration of Illness	-	-	14.64	11.02	-	-
Current Symptomatology						
Depression (HAMD)	0.30	0.72	3.57	3.68	6*	<.001
Mania (YMRS)	0.17	0.48	2.66	3.53	4.78*	<.001
Psychosis (BPRS)	24.53	0.91	28.24	4.07	6.12*	<.001
Medications, n (%)						
Mood stabilizer(s)	-	-	52.24		-	-
Antidepressant(s)	-	-	41.79		-	-
Atypical Antipsychotic(s)	-	-	32.84		-	-
Anxiolytic/Benzodiazepine(s)	-	-	34.33		-	-
Lithium	-	-	14.93		-	-
Unmedicated	-	-	16.42		-	-
Typical Antipsychotic(s)	-	-	1.49		-	-
Co-morbid Diagnoses, n (%)						
Anxiety	-	-	44.78		-	-
Alcohol	-	-	58.21		-	-
Drug use history	-	-	41.79		-	-

Table S3. Bipolar Illness Sample Demographics. BPRS, Brief Psychiatric Rating Scale; HAMD, Hamilton Depression rating scale; Hx, history; YMRS, Young Mania Rating Scale; M, Mean; SD, Standard Deviation; age, education levels, parental education, age at diagnosis and duration of illness are expressed in years. * denotes a significant T statistic for the between-group t-test. Given different diagnostic and assessment needs for schizophrenia and bipolar illness there are some differences in clinical instruments used to characterize the clinical samples. For complete clinical details and clinical measure descriptions used for the bipolar sample please refer to our prior work (Anticevic *et al.* 2012).

Table S4 | Clinical and Demographic Characteristics - Schizophrenia Replication Sample

Characteristic	Controls (N=23)		Patients (N=23)		Significance	
	M	S.D.	M	S.D.	T Value / Chi-Square	P Value (two-tailed)
Age (in years)	37.18	7.59	36.39	9.54	.31	.76
Gender (% male)	74		78		.34	.73
Paternal education (in years)	12.70	1.46	13.26	2.61	.9	.37
Maternal education	12.48	1.53	13.50	3.07	1.42	.16
Paternal SES	21.59	8.92	26.59	10.73	1.67	.1
Maternal SES	17.27	8.55	25.24	11.88	2.51*	<.02
Participant's education (in years)	15.26	2.12	13.04	2.14	3.5*	<.001
Handedness (% right)	100.00		86.96		1.45	.15
IQ Verbal	110.23	10.85	95.23	14.18	3.88*	<.001
IQ Performance	115.45	11.64	101.82	15.24	3.3*	<.01
Medication (CPZ equivalents)	-	-	584.63	563.63	-	-
Mean SAPS Global Item Score	-	-	1.91	1.21	-	-
Mean SANS Global Item Score	-	-	2.50	0.78	-	-
Disorganization	-	-	5.48	2.71	-	-
Poverty	-	-	10.43	3.53	-	-
Reality Disotortion	-	-	4.26	3.53	-	-

Table S4. Schizophrenia Replication Sample Demographics. Positive symptoms were the sum of global scores for hallucinations and delusions; negative symptoms were the sum of global scores for alogia, anhedonia, avolition, affective flattening, and attentional impairment; and disorganization symptoms were the sum of global scores for bizarre behavior, positive thought disorder, and inappropriate affect. SAPS, scale for assessment of positive symptoms; SANS, scale for the assessment of negative symptoms; CPZ, chlorpromazine; SES, socioeconomic status; M, Mean; SD, Standard Deviation; IQ, intelligence quotient; age, education levels, parental education, and age are expressed in years. * denotes a significant T statistic for the between-group t-test. The smaller schizophrenia replication sample reported here was characterized and reported previously in the context of our prior work (Anticevic *et al.* 2011; Cole *et al.* 2011).

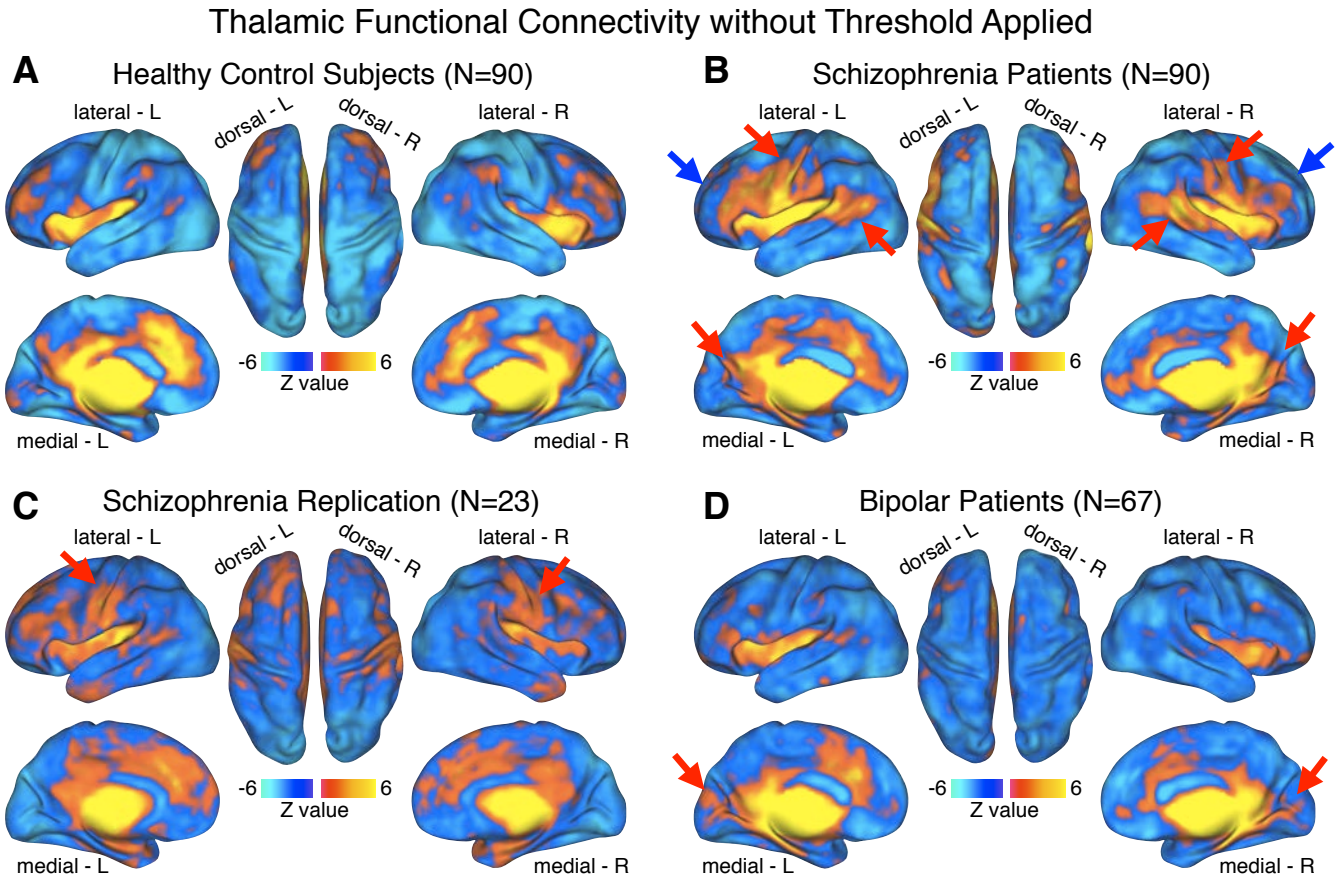

Figure S1. Unthresholded Thalamic Functional Connectivity Patterns Across Groups. We highlight thalamic connectivity at the whole-brain level for **(A)** control subjects in the discovery sample (N=90); and **(B)** individuals with schizophrenia in the discovery sample (N=90); **(C)** individuals with schizophrenia in the replication sample (N=23); and **(D)** individuals with bipolar illness (N=67). The key aim of this unthresholded analysis was to facilitate visual inspection of normative and patient connectivity patterns in the absence of a direct contrast. In addition to shifted connectivity distribution plots (**Figures 2 & S3**), these patterns support the conclusion that there is indeed a quantitative upward and downward shift in connectivity across certain sensory (red arrows) and prefrontal/cerebellar nodes (blue arrows) respectively, which is also evident in the replication sample (although to a lesser extent, perhaps due to reduced sample size). Bipolar patents showed qualitatively less 'severe' connectivity shifts as compared to the two schizophrenia samples (also evident in **Figure S3**). Overall, whole-brain patterns of thalamic coupling for control participants generally replicate prior resting-state findings in the literature (Zhang et al. 2010). For a complete pattern of group difference contrast maps see **Figure S2**.

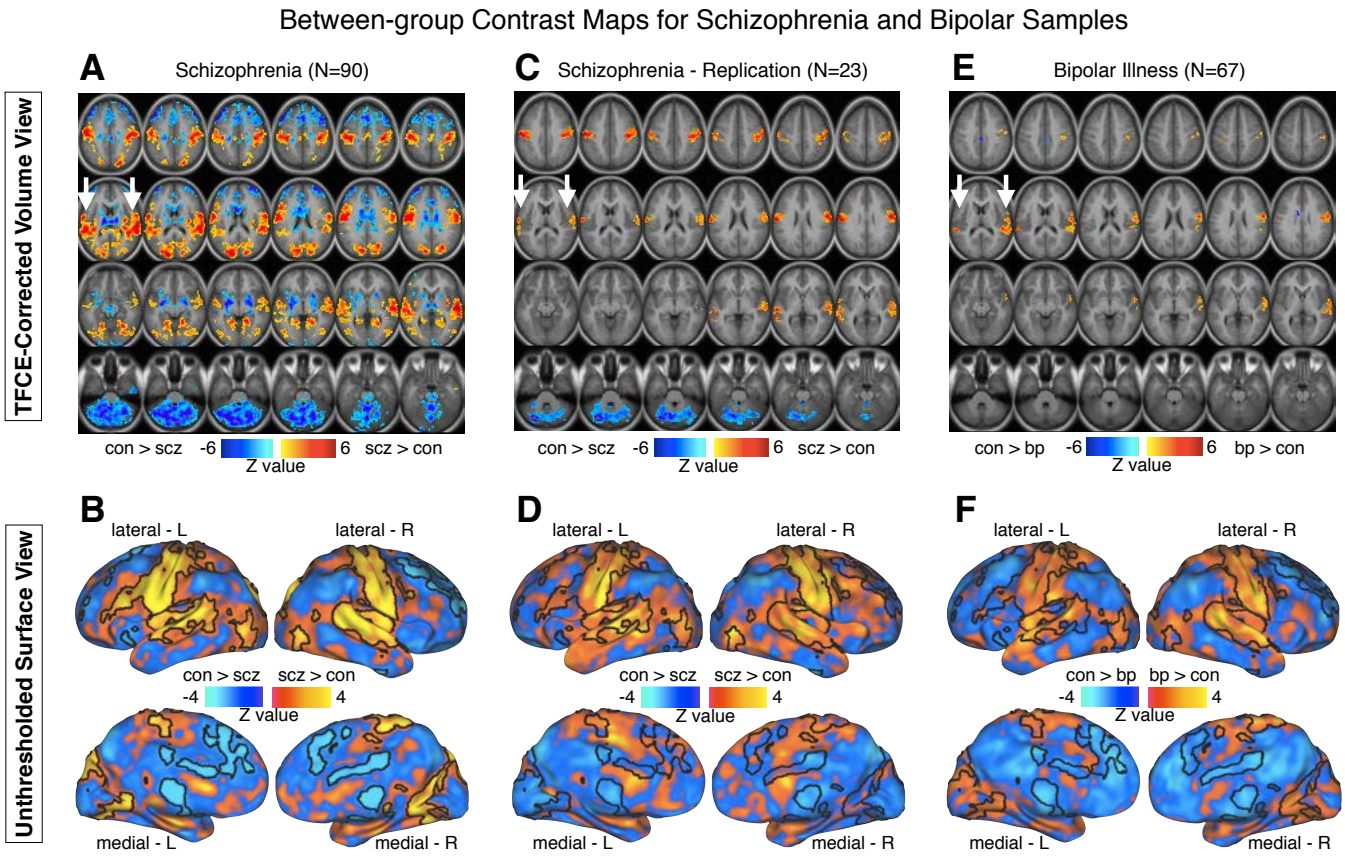

Figure S2. Between-group Thalamic Connectivity Contrast Maps. (A) Threshold-free cluster enhancement (TFCE) (Smith and Nichols 2009) whole-brain corrected volume map of group differences between patients with schizophrenia (SCZ) and matched control subjects (CON) for the discovery sample (N=90), as in **Figure 1**. **(B)** Unthresholded surface contrast map of group differences between SCZ and CON with TFCE-corrected regions outlined with black borders. **(C)** TFCE-corrected volume map of group differences between an independent sample of SCZ and CON (N=23 per group). Given statistical independence, analyses were computed within the mask of regions showing group differences for the discovery schizophrenia sample. **(D)** Between-group unthresholded surface contrast map for the schizophrenia replication sample. Again, TFCE-corrected regions from the discovery sample are outlined with black borders for comparison (as in panel B). **(E)** TFCE-corrected map of group differences between bipolar patients (BP) (N=67) and their respective matched controls (CON) (N=47). Again, given statistical independence, analyses were computed within the mask of regions showing group differences for the discovery schizophrenia sample. **(F)** Between-group unthresholded surface contrast map for the bipolar sample. Again, TFCE-corrected regions from the schizophrenia discovery sample are outlined with black borders for comparison (as in panels B & D).

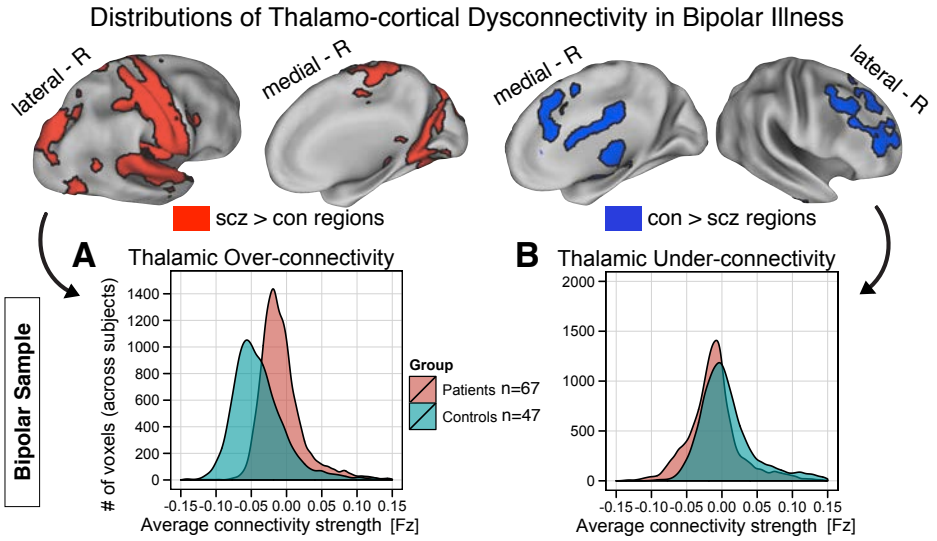

Figure S3. Distributions of Thalamo-cortical Connectivity for Bipolar Illness. As in the main text (**Figure 2**), top panels show regions for which we identified increased (red) and decreased (blue) thalamic connectivity in schizophrenia using the discovery sample (N=90). Given statistical independence, here we used these exact regions to extract distribution plots for the bipolar sample (N=67) and their respective matched controls (N=47). **(A)** Distributions of average connection strengths for bipolar patients relative to controls across voxels identified as showing increased thalamic connectivity in the original analysis. **(B)** Distributions of average connection strengths for bipolar patients relative to controls across voxels identified as showing reduced thalamic connectivity in the original analysis. Similar to schizophrenia findings across two independent samples (**Figure 2**), there was a shift across both distributions for bipolar patients. However, the between-group distribution plots indicates less prominent shifts for bipolar individuals relative to perturbations observed in schizophrenia (see **Figure 3**) (between-group contrast maps for the bipolar sample are shown in **Figure 6E** and **Figure S2E-F**, threshold-free thalamic coupling for the bipolar sample is shown in **Figure S1D**, whereas schizophrenia-bipolar contrast maps are shown in **Figure S4**).

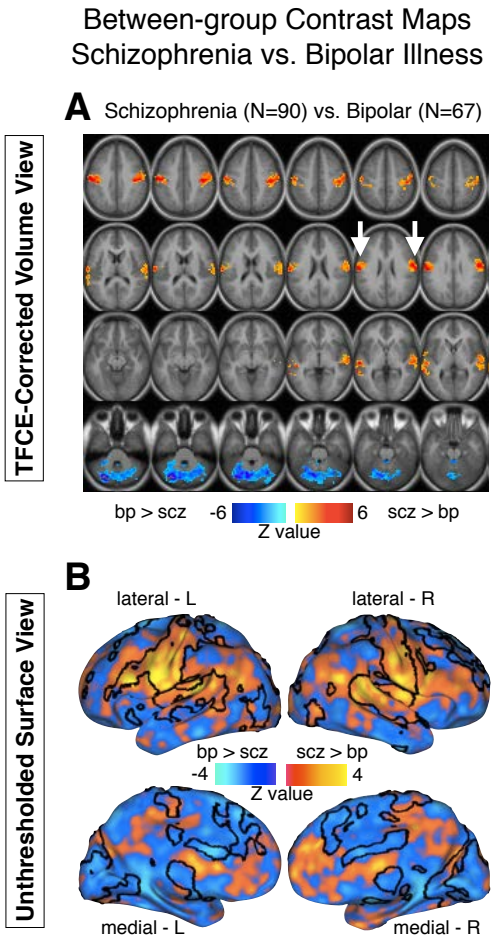

Figure S4. Between-group Thalamic Connectivity Contrast Maps for Schizophrenia vs. Bipolar Patients. (A) Threshold-free cluster enhancement (TFCE) corrected volume map of group differences between patients with schizophrenia (SCZ) and bipolar patients (BP) within the mask identified for the discovery sample (as in **Figure 1**). **(B)** Unthresholded surface contrast map of group differences between SCZ and BP with TFCE-corrected regions from the original discovery sample outlined with black borders. Note: We acknowledge that schizophrenia and bipolar samples studied here were not explicitly matched for a between-group comparison (bipolar patients were in remission, while schizophrenia patients were quite symptomatic). Therefore, this finding, despite large sample sizes, should be expanded upon in clinical neuroimaging studies explicitly designed to directly compare patients diagnosed with the two illnesses, and as such should be interpreted as provisional (see Limitations).

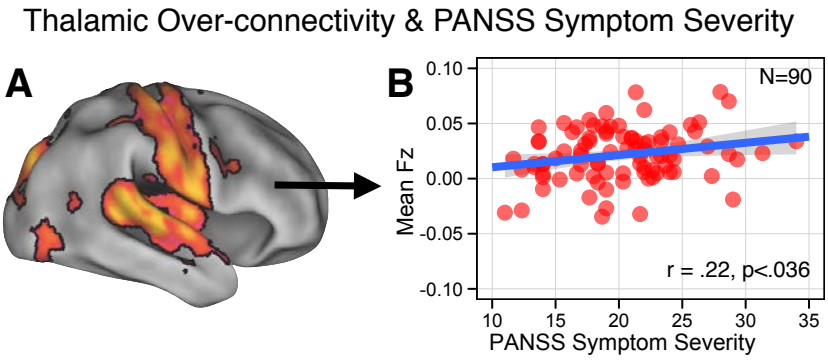

Figure S5. Relationship Between Symptoms and Thalamic Over-connectivity. (A) Regions where schizophrenia patients exhibited stronger thalamic connectivity, centered on sensory-motor cortices. **(B)** Significant positive relationship between thalamic connectivity across all voxels in panel A and overall PANSS symptom severity for schizophrenia patients (N=90, r=.22, p<.036).

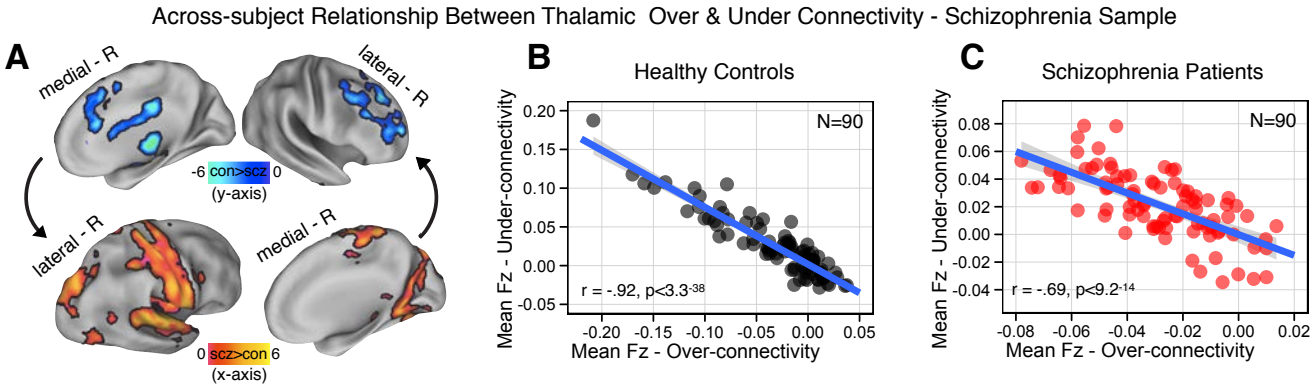

Figure S6. Relationship Between Thalamic Over & Under-connectivity in Schizophrenia. (A) Regions showing reduced (blue foci, top panel) vs. increased (orange-red foci, bottom panel) thalamic coupling in schizophrenia (as **Figure 1A**). We extracted mean thalamic functional connectivity out of these regions for each subject. **(B)** Across healthy subjects (N=90) thalamic coupling of these two systems was negatively correlated (r=-.92, $p<3.3^{-38}$). **(C)** Across schizophrenia patients (N=90) a significant negative relationship was evident (r=-.69, $p<9.2^{-14}$), but was significantly reduced relative to healthy controls ($p<4.2^{-7}$). Analyses for bipolar patients (N=67) and matched controls (N=47) (**Figure S7)** revealed highly significant negative relationships (Bipolar: r=-.83, $p<4.8^{-18}$; Controls: r=-.82, $p<3.1^{-12}$), which did not differ. Analyses across all subjects (N=340), further suggest reduced differentiation and coherence between thalamo-cortical systems in schizophrenia (see **Figure 3**).

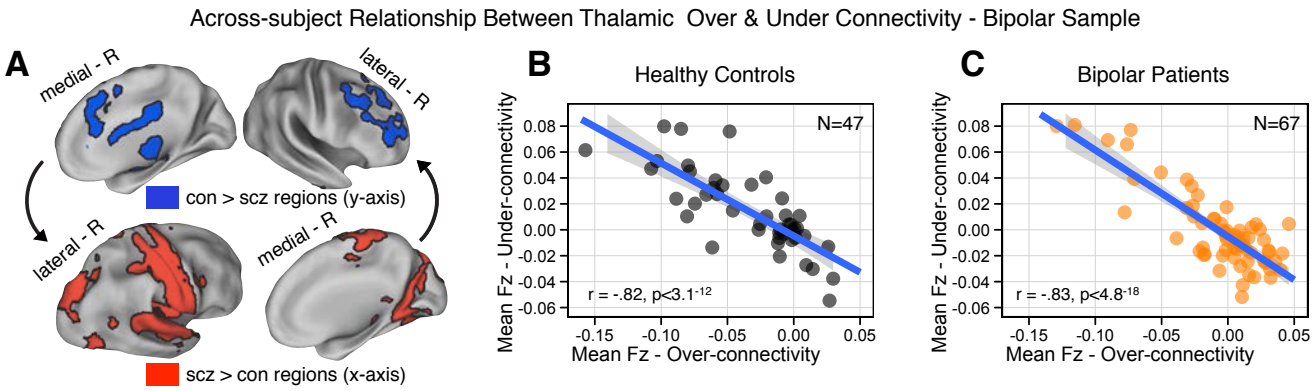

Figure S7. Relationship Between Thalamic Over & Under-connectivity in Bipolar Illness. (A) As in the main text (**Figure 3**), panels show regions for which we identified reduced (blue, top panel) and increased (red, bottom panel) thalamic connectivity in schizophrenia using the original discovery sample (N=90). As before, given statistical independence, we extracted signal out of these regions for each subject across all voxels for the bipolar sample (N=67) and their respective matched controls (N=47). **(B)** As for the discovery sample, across all healthy control subjects (N=47) the systems showing increased (x-axis) vs. decreased (y-axis) coupling pattern with the thalamus were highly negatively correlated ($r=-.82$, $p<3.1^{-12}$), replicating the independent analysis discovery analyses (**Figure S6**). **(C)** The same pattern was identified for the bipolar sample ($r=-.83$, $p<4.8^{-18}$). Critically, unlike results for the schizophrenia discovery sample (see **Figure S6**), these correlation coefficients did not differ between groups ($p=.27$, NS) (in fact, bipolar group was slightly numerically higher). Together, these additional validations across independent samples of healthy controls and bipolar patients suggest that systems showing increased/reduced thalamic connectivity in schizophrenia are likely not independent sources of thalamo-cortical disturbances and seem to be a stable property of thalamo-cortical systems. Moreover, the reductions in thalamo-cortical system relationships seem to be more profound in schizophrenia, highlighting the possibility for a reduced coherence between thalamo-cortical systems in this illness (see **Figure 3** for an expanded analysis across all subjects).

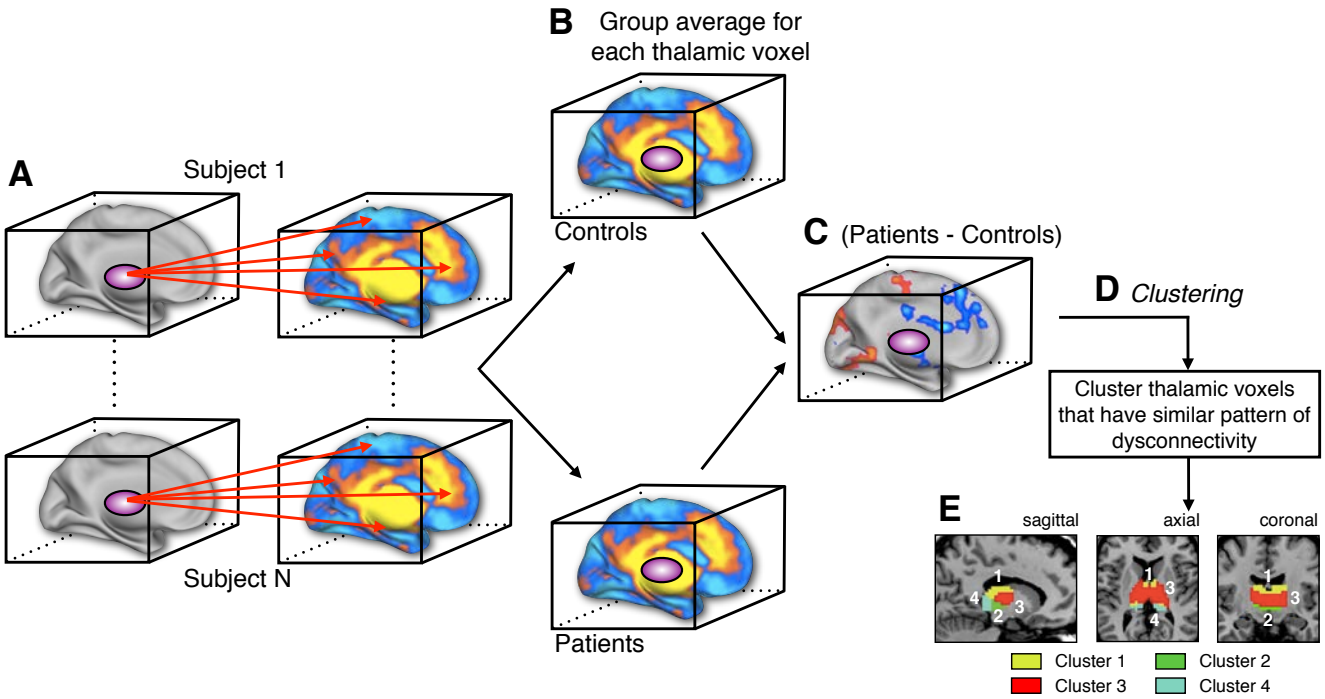

Figure S8. Visual Illustration of Thalamic Clustering Method & Workflow. (A) First, thalamic connectivity was computed for each subject such that each thalamic voxel is correlated with all other gray matter voxels, providing a comprehensive voxel-wise thalamic connectivity map for each subject. This process is then repeated for each subject across both groups. **(B)** Average group-based thalamic connectivity maps are computed where for each thalamic voxel its average connectivity is calculated across subjects within a given group for all gray matter voxels. **(C)** Group difference (i.e. dysconnectivity) maps between patient and healthy control group average thalamic connectivity maps are computed for each voxel. This group-differenced thalamic connectivity map is then used for clustering. **(D)** Clustering is then performed on the difference maps of group-based average thalamic connectivity such that voxels with 'similar' patterns of group differences are grouped together into a given cluster. **(E)** Ultimately, this procedure produces clusters of voxels with similar dysconnectivity patterns. Note: all functional surface maps shown here (panels A-C) are purely illustrative and used as visual examples in the workflow.

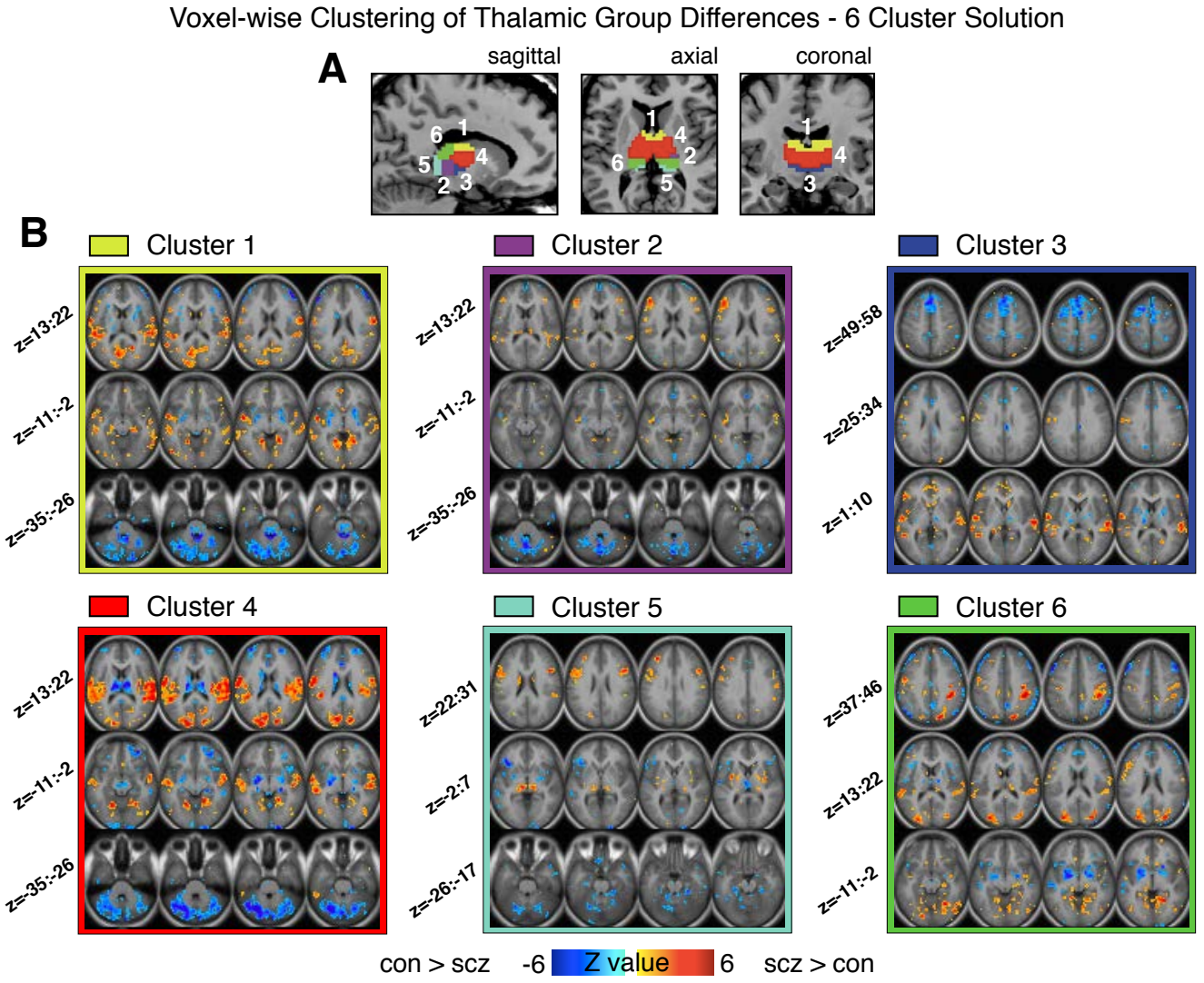

Figure S9. Voxel-wise Clustering of Group Differences in Thalamic Connectivity: 6 Cluster Solution. (A) Clustering patterns of between-group thalamic connectivity differences for a 6-cluster solution (for a 4-cluster solution see **Figure 5**). **(B)** Maps of between-group differences across all 6 clusters when a specific cluster is used as a seed. As evident from the maps, the pattern of between-group differences for cluster #4 (red) was most similar to those when examining the entire thalamus (see **Figure 1**), which again roughly corresponds to higher-order associative thalamic nodes (Behrens *et al.* 2003). Notably, irrespective of cluster solution (either 4 or 6 cluster), findings indicate a specific cluster (shown in red across both figures) that exhibits highest correspondence with overall group results. To quantify this effect, we also computed formal similarity (eta^2) between both cluster solutions and anatomically defined between-group thalamic maps (see **Figure S11**). Z coordinate ranges for each row of slices are shown next to each cluster panel (each axial slice in each row increments by 3mm). Note: all group difference connectivity maps are shown at $p<0.01$ ($Z>2.33$) uncorrected to allow full qualitative inspection of patterns.

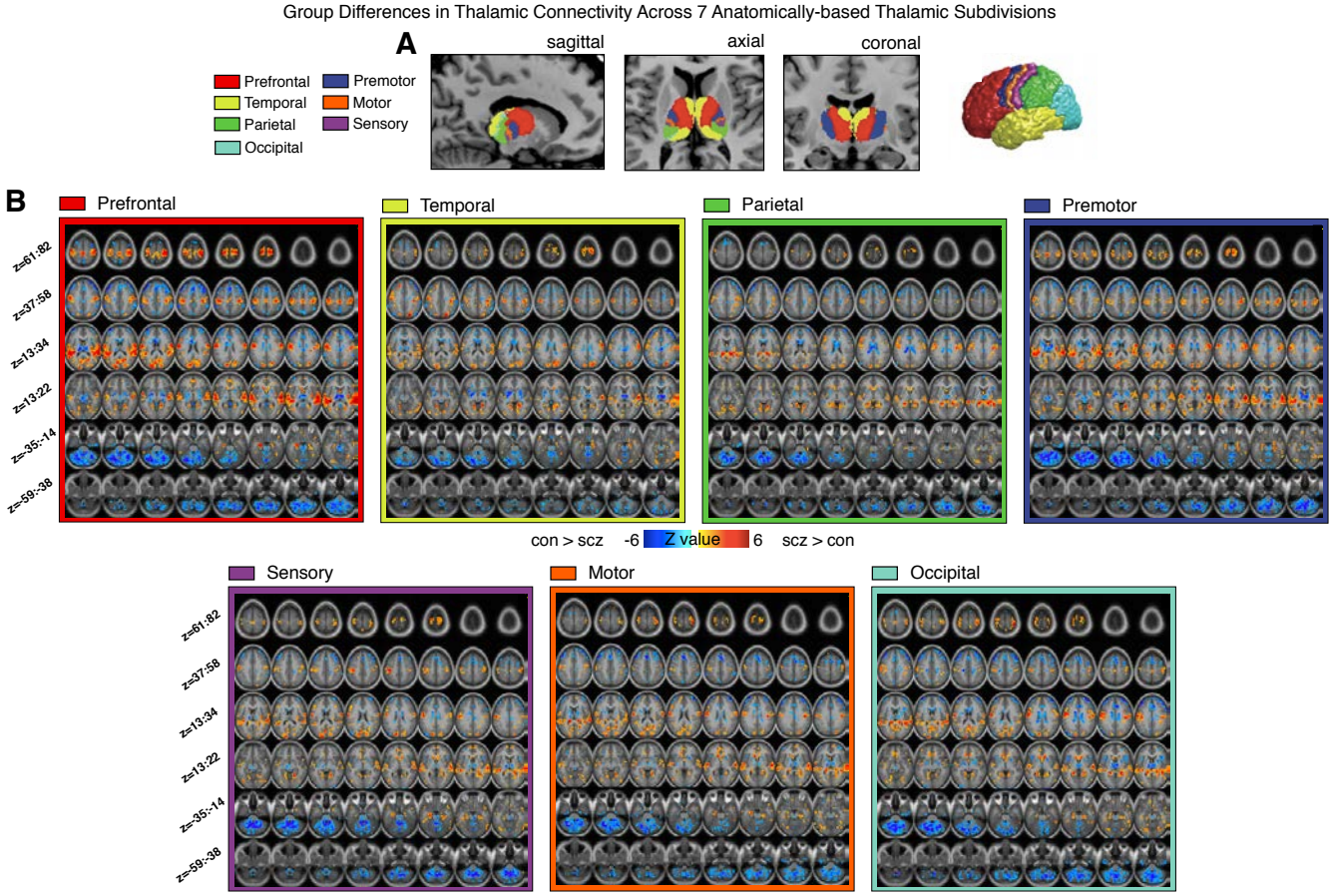

Figure S10. Group Differences in Thalamic Connectivity Across 7 Anatomically-based Thalamic Subdivisions. (A) Thalamus subdivisions based on the FSL thalamic atlas are shown to further facilitate examination of how data-driven dysconnectivity follows anatomy. Right: adapted with permission from Johansen-Berg and colleagues (Johansen-Berg *et al.* 2005), we illustrate cortical sectors showing different patterns of thalamic anatomical connectivity. **(B)** Maps of between-group differences across all 7 anatomically-based thalamic clusters when a specific cluster is used as a seed. As evident from the maps, the pattern of between-group differences for anatomic cluster #1 (red) was most similar to those when examining the entire thalamus (see **Figure 1**), which corresponds to the thalamic subdivision with dense projections to prefrontal cortex (Behrens *et al.* 2003). As noted, to quantify this effect, we also computed formal similarity (eta^2) between all data-driven cluster solutions and anatomically defined between-group thalamic maps (see **Figure S11**). Z coordinate ranges for each row of slices are shown next to each cluster panel (each axial slice in each row increments by 3mm). Note: all group difference connectivity maps are shown at $p<0.01$ ($Z>2.33$) uncorrected to allow full qualitative inspection of patterns.

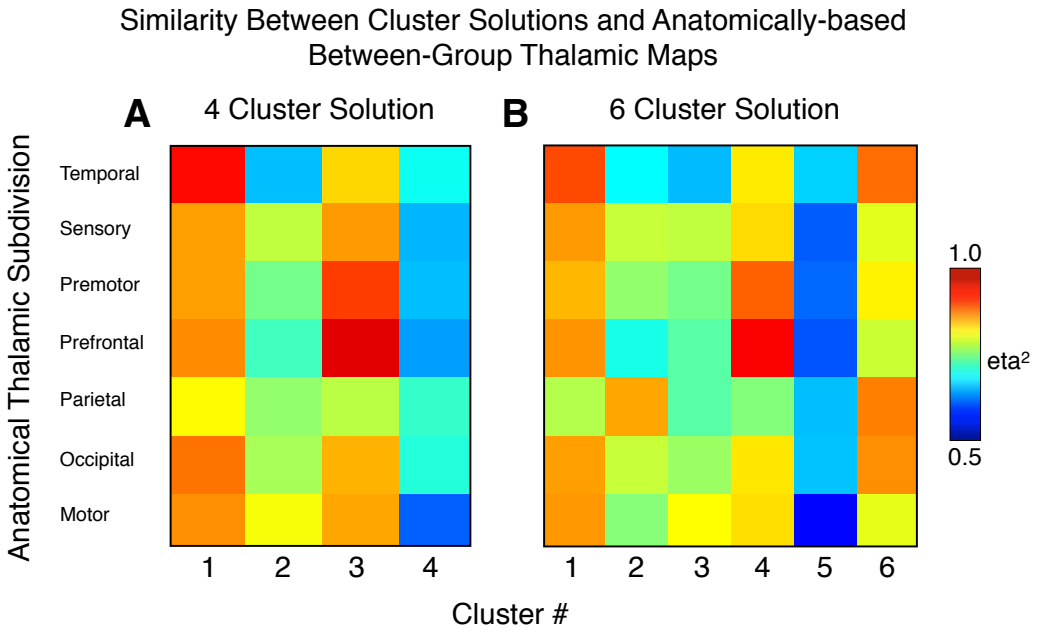

Figure S11. Similarity Between Cluster Solutions and Anatomically-based Between-group Thalamic Maps. Complete matrix of similarity between each group difference map across anatomically-defined thalamic subdivisions (y-axis) and each cluster across **(A)** 4-cluster and **(B)** 6-cluster solutions (x-axes). Each color-coded square across the two matrixes represents eta^2, expressed using a heat map where brighter red values indicate higher similarity, whereas blue-green values indicate lower similarity. Prefrontal and premotor thalamic node similarity with cluster 3 in panel A (and cluster 4 in panel B) indicate that patterns of dysconnectivity for patients vs. controls were highly similar across these seeds, as indexed by a high eta^2 index. By contrast, the data-driven clusters 4 and 5 across panels A & B respectively showed relatively lower similarity when compared to all anatomically derived thalamic seeds, suggesting that this particular cluster solution may not strictly follow anatomically-defined thalamic boundaries. Overall, the key effect highlighted across both panels A & B suggests that thalamic nuclei known to project densely to prefrontal cortex show a high degree of similarity with clusters 3 (in panel A) and 4 (in panel B).

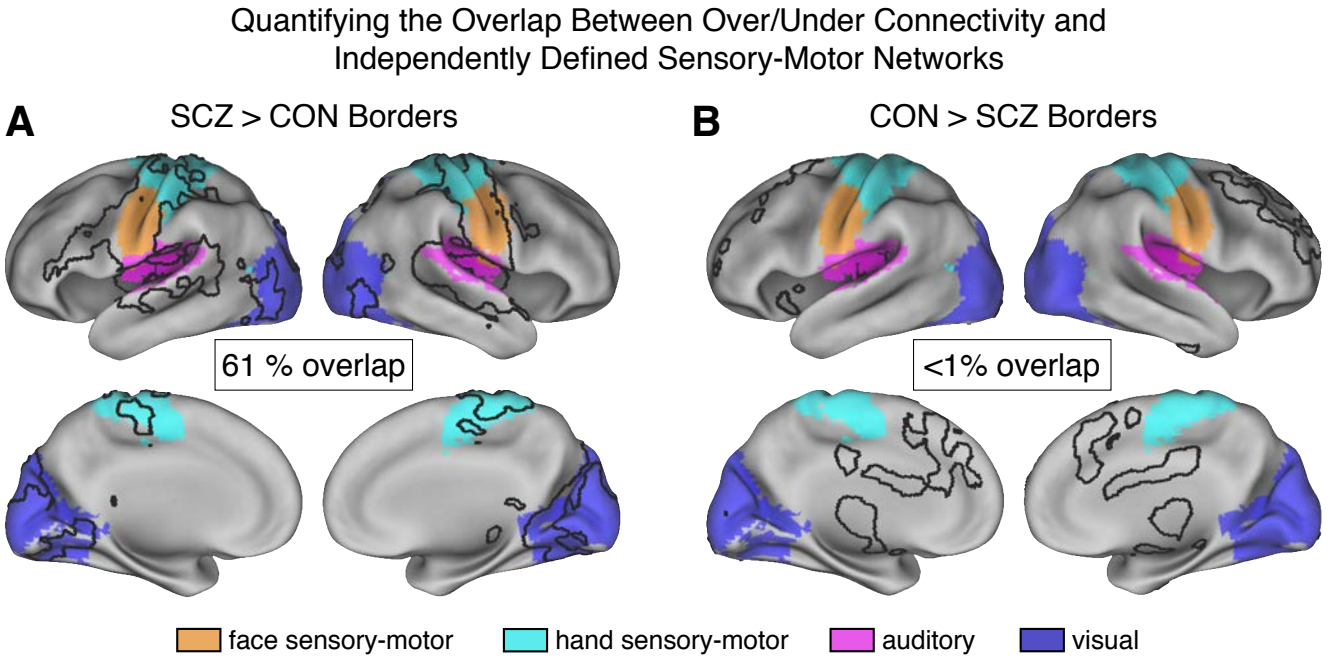

Figure S12. Quantifying the Overlap between Over/Under Connectivity and Independently Defined Sensory-Motor Networks. Given the striking correspondence between areas showing thalamic over-connectivity in schizophrenia and sensory-motor cortices we explicitly quantified whether present findings fall within sensory-motor networks. To accomplish this, we used the sensory-motor network map defined independently via resting-state by Power and colleagues (2011) (obtained with permission from (Power et al. 2011)). **(A)** As noted in the main text, 61% of all voxels identified as over-connected with the thalamus in patients (black borders) overlapped with the sensory-motor network boundaries (visualized via color-coded maps). **(B)** In contrast, less than 1% of all voxels identified as under-connected with the thalamus in schizophrenia (black borders) fell within the sensory-motor network boundaries. To confirm this statistically we ran a binomial test for proportions: 61% of spatial overlap between the two maps significantly exceeded the proportion expected by chance alone ($p<0.000001$, binomial test for proportions). Similarly, the observation that almost all of the under-connected voxels fell outside of the sensory-motor maps also exceeded chance ($p<0.000001$), as by chance alone we would expect approximately ~17% overlap (given the number of voxels in the sensory-motor networks relative to all possible voxels).

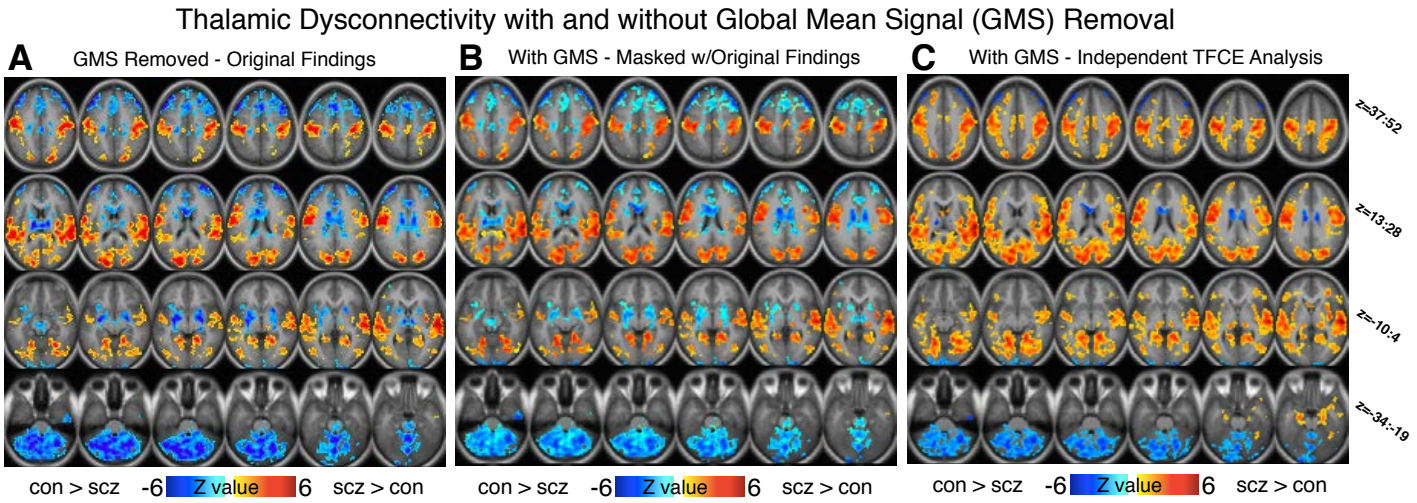

Figure S13. Thalamic Dysconnectivity with and without Global Mean Signal (GMS) Removal. Given that GMS removal is a key consideration in functional connectivity work, we repeated the analyses without this step to verify that patterns remained unchanged. **(A)** Original results with GMS removed to allow qualitative inspection of patterns across analyses. We conducted two additional analyses without GMS removal: **(B)** Results within the originally identified mask to allow qualitative inspection of the pattern within the originally defined regions; **(C)** We repeated the entire TFCE-corrected analysis using identical permutation testing for the between-group results as in the main text. Here we juxtapose both results next to the original findings to allow qualitative inspection. The general pattern of results remained unchanged; however, there were some subtle differences, particularly within prefrontal regions that future studies should explore further. These discrepancies however did not reflect a qualitative difference in patterns (as panel B shows a highly similar pattern within the original mask without GMS removal).

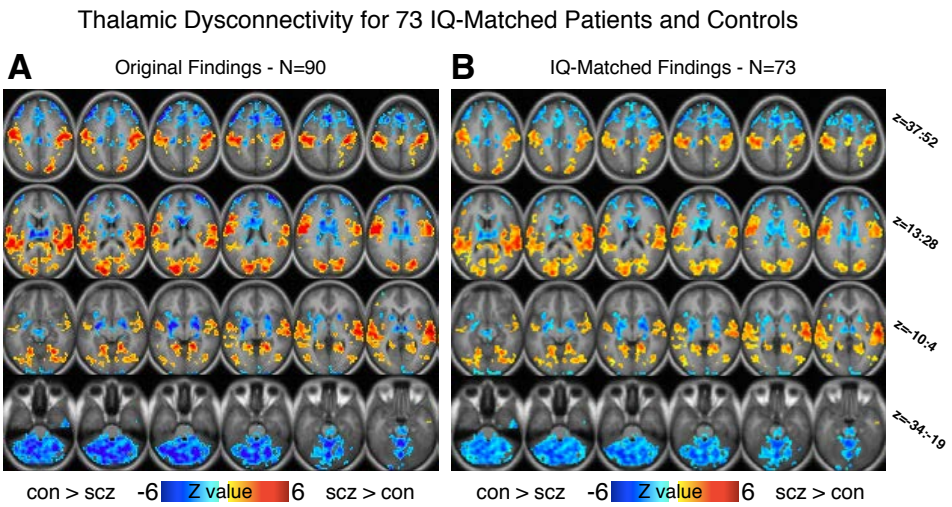

Figure S14. Thalamic Dysconnectivity for 73 IQ-Matched Patients and Controls. (A) Original results across N=90 subjects to allow quick inspection of similarities across analyses. **(B)** Results for a subset of N=73 subjects that were explicitly matched for IQ across groups and all other variables as done for the original analysis. To facilitate inspection, results were masked within regions identified originally (panel A), illustrating virtually no qualitative differences when groups were matched on the measures of premorbid intellectual functioning used in the present investigation. However, as noted above, it is important to acknowledge that the 'IQ' measures used here likely do not reflect the complex nature of cognitive deficits in schizophrenia. Therefore, it will be vital for future studies to explicitly relate present effects to more comprehensive measures of higher cognitive function in this illness (Barch and Ceaser 2012).

Supplementary References

Andreasen NC, Pressler M, Nopoulos P, Miller D, Ho B-C. 2010. Antipsychotic dose equivalents and dose-years: a standardized method for comparing exposure to different drugs. Biol Psychiatry. 67:255-262.

Anticevic A, Brumbaugh MS, Winkler AM, Lombardo LE, Barrett J, Corlett PR, Kober H, Gruber J, Repovs G, Cole MW, Krystal JH, Pearlson GD, Glahn DC. 2012. Global Prefrontal and Fronto-amygdala Dysconnectivity in Bipolar I Disorder with Psychosis History. Biol Psychiatry. 73:565-573.

Anticevic A, Repovs G, Corlett PR, Barch DM. 2011. Negative and Non-emotional Interference with Visual Working Memory in Schizophrenia. Biol Psychiatry. 70:1159-1168.

Anticevic A, Repovs G, Van Snellenberg JX, Csernansky JG, Barch DM. 2010. Subcortical alignment precision in patients with schizophrenia. Schizophr Res. 120:76-83.

Barch DM, Ceaser A. 2012. Cognition in schizophrenia: core psychological and neural mechanisms. Trends In Cognitive Sciences. 16:27-34.

Behrens TE, Johansen-Berg H, Woolrich MW, Smith SM, Wheeler-Kingshott CA, Boulby PA, Barker GJ, Sillery EL, Sheehan K, Ciccarelli O, Thompson AJ, Brady JM, Matthews PM. 2003. Non-invasive mapping of connections between human thalamus and cortex using diffusion imaging. Nat Neurosci. 6:750-757.

Cauda F, D'Agata F, Sacco K, Duca S, Geminiani G, Vercelli A. 2011. Functional connectivity of the insula in the resting brain. Neuroimage. 55:8-23.

Chang C-C, Lin C-J. 2011. LIBSVM: A library for support vector machines. ACM Transactions on Intelligent Systems and Technology. 2:1:27.

Cohen AL, Fair DA, Dosenbach NU, Miezin FM, Dierker D, Van Essen DC, Schlaggar BL, Petersen SE. 2008. Defining functional areas in individual human brains using resting functional connectivity MRI. Neuroimage. 41:45-57.

Cole MW, Anticevic A, Repovs G, Barch DM. 2011. Variable global dysconnectivity and individual differences in schizophrenia. Biol Psychiatry. 70:43-50.

First MB, Spitzer RL, Miriam G, Williams JBW. 2002. Structured clinical interview for DSM-IV-TR Axis I Disorders, Research Version, Non-patient Edition (SCID-I/NP). New York: Biometrics Research, New York State Psychiatric Institute.

Gelman A, Hill J. 2007. Missing-data imputation. In: Data Analysis Using Regression and Multilevel/Hierarchical Models New York: Cambridge University Press p 529-543.

Glahn DC, Bearden CE, Bowden CL, Soares JC. 2006. Reduced educational attainment in bipolar disorder. J Affect Disord. 92:309–312.

Goldman-Rakic. 1995. Cellular basis of working memory. Neuron. 14:477-485.

Johansen-Berg H, Behrens TE, Sillery E, Ciccarelli O, Thompson AJ, Smith SM, Matthews PM. 2005. Functional-anatomical validation and individual variation of diffusion tractography-based segmentation of the human thalamus. Cereb Cortex. 15:31-39.

Klein A, Andersson J, Ardekani BA, Ashburner J, Avants B, Chiang MC, Christensen GE, Collins DL, Gee J, Hellier P, Song JH, Jenkinson M, Lepage C, Rueckert D, Thompson P, Vercauteren T, Woods RP, Mann JJ, Parsey RV. 2009. Evaluation of 14 nonlinear deformation algorithms applied to human brain MRI registration. Neuroimage. 46:786-802.

Krystal JH, D'Souza DC, Gallinat J, Driesen NR, Abi-Dargham A, Petrakis I, Heinz A, Pearlson GD. 2006. The vulnerability to alcohol and substance abuse in individuals diagnosed with schizophrenia. Neurotox Res. 10:235-252.

LaBar KS, Gitelman DR, Mesulam MM, Parrish TB. 2001. Impact of signal-to-noise on functional MRI of the human amygdala. Neuroreport. 12:3461-3464.

Nanetti L, Cerliani L, Gazzola V, Renken R, Keysers C. 2009. Group analyses of connectivity-based cortical parcellation using repeated k-means clustering. Neuroimage. 47:1666-1677.

Parnaudeau S, O'Neill PK, Bolkan SS, Ward RD, Abbas AI, Roth BL, Balsam PD, Gordon JA, Kellendonk C. 2013. Inhibition of mediodorsal thalamus disrupts thalamofrontal connectivity and cognition. Neuron. 77:1151-1162.

Parrish TB, Gitelman DR, LaBar KS, Mesulam MM. 2000. Impact of signal-to-noise on functional MRI. Magn Reson Med. 44:925-932.

Power JD, Barnes KA, Snyder AZ, Schlaggar BL, Petersen SE. 2012. Spurious but systematic correlations in functional connectivity MRI networks arise from subject motion. Neuroimage. 59:2142-2154.

Power JD, Cohen AL, Nelson SM, Wig GS, Barnes KA, Church JA, Vogel AC, Laumann TO, Miezin FM, Schlaggar BL, Petersen SE. 2011. Functional network organization of the human brain. Neuron. 72:665-678.

Smith SM, Nichols TE. 2009. Threshold-free cluster enhancement: addressing problems of smoothing, threshold dependence and localisation in cluster inference. Neuroimage. 44:83-98.

Spreen O, Strauss E. 1998. A compendium of neuropsychological tests: Administration, norms, and commentary. New York: Oxford University Press.

Zhang D, Snyder AZ, Shimony JS, Fox MD, Raichle ME. 2010. Noninvasive functional and structural connectivity mapping of the human thalamocortical system. Cereb Cortex. 20:1187-1194.